

Polarization measurement of laser-accelerated protons

Natascha Raab, Markus Büscher, Mirela Cerchez, Ralf Engels, Ilhan Engin, Paul Gibbon, Patrick Greven, Astrid Holler, Anupam Karmakar, Andreas Lehrach, Rudolf Maier, Marco Swantusch, Monika Toncian, Toma Toncian, and Oswald Willi

Citation: *Physics of Plasmas* (1994-present) **21**, 023104 (2014); doi: 10.1063/1.4865096

View online: <http://dx.doi.org/10.1063/1.4865096>

View Table of Contents: <http://scitation.aip.org/content/aip/journal/pop/21/2?ver=pdfcov>

Published by the [AIP Publishing](#)

Articles you may be interested in

[Proton trajectories and electric fields in a laser-accelerated focused proton beam](#)

Phys. Plasmas **19**, 056702 (2012); 10.1063/1.3700181

[Magnetic field measurements in laser-produced plasmas via proton deflectometry](#)

Phys. Plasmas **16**, 043102 (2009); 10.1063/1.3097899

[Laser beam-profile impression and target thickness impact on laser-accelerated protons](#)


Phys. Plasmas **15**, 053101 (2008); 10.1063/1.2912451


[Plasma Diagnostics of a Forward Laser Plasma Accelerated Thruster](#)

AIP Conf. Proc. **830**, 201 (2006); 10.1063/1.2203263


[The generation of micro-fiducials in laser-accelerated proton flows, their imaging property of surface structures and application for the characterization of the flow](#)

Phys. Plasmas **11**, L17 (2004); 10.1063/1.1690302

A collection of five pieces of Pfeiffer Vacuum equipment, including a red turbopump, a silver turbopump, a white turbopump, a red turbopump with a long shaft, and a silver chamber component.

 Vacuum Solutions from a Single Source

- Turbopumps
- Backing pumps
- Leak detectors
- Measurement and analysis equipment
- Chambers and components

PFEIFFER  **VACUUM**

Polarization measurement of laser-accelerated protons

Natascha Raab,^{1,a)} Markus Buescher,^{1,2,3,b)} Mirela Cerchez,³ Ralf Engels,¹ Ilhan Engin,¹ Paul Gibbon,⁴ Patrick Greven,¹ Astrid Holler,¹ Anupam Karmakar,^{4,c)} Andreas Lehrach,¹ Rudolf Maier,¹ Marco Swantusch,³ Monika Toncian,³ Toma Toncian,³ and Oswald Willi³

¹Institut für Kernphysik and Jülich Center for Hadron Physics, Forschungszentrum Jülich, 52425 Jülich, Germany

²Peter Grünberg Institut (PGI-6), Forschungszentrum Jülich, 52425 Jülich, Germany

³Institute for Laser- and Plasma Physics, Heinrich-Heine Universität Düsseldorf, Universitätsstr. 1, 40225 Düsseldorf, Germany

⁴Institute for Advanced Simulation, Jülich Supercomputing Centre, Forschungszentrum Jülich, 52425 Jülich, Germany

(Received 24 November 2013; accepted 28 January 2014; published online 12 February 2014)

We report on the successful use of a laser-driven few-MeV proton source to measure the differential cross section of a hadronic scattering reaction as well as on the measurement and simulation study of polarization observables of the laser-accelerated charged particle beams. These investigations were carried out with thin foil targets, illuminated by 100 TW laser pulses at the Arcturus laser facility; the polarization measurement is based on the spin dependence of hadronic proton scattering off nuclei in a Silicon target. We find proton beam polarizations consistent with zero magnitude which indicates that for these particular laser-target parameters the particle spins are not aligned by the strong magnetic fields inside the laser-generated plasmas. © 2014 Author(s). All article content, except where otherwise noted, is licensed under a Creative Commons Attribution 3.0 Unported License. [<http://dx.doi.org/10.1063/1.4865096>]

I. INTRODUCTION

The field of laser-induced relativistic plasmas and, in particular, of laser-driven particle acceleration, has undergone impressive progress in recent years.¹ Despite many advances in the understanding of fundamental physical phenomena, one unexplored issue is how the particle spins are influenced by the huge magnetic fields inherently present in the plasmas.^{2–5} There are two mechanisms which can potentially cause a polarization of the particle beam: either due to a spin alignment or by spatial separation of different spin states induced by gradients in the magnetic field of the plasma. The second scenario relies on the same principle as the Stern-Gerlach experiment⁶ in which a beam of neutral Silver atoms is deflected in an inhomogeneous magnetic field depending on the spin state of the valence electron.

On the other hand, according to the “thesis of Bohr,”⁷ the spin states of free electrons, or any other charged particle, cannot be separated in a Stern-Gerlach like set-up, since the spatial uncertainty of the charged particle along the direction of the magnetic gradient leads to an uncertainty in the Lorentz force of the same order of magnitude as the force that divides the spin states. However, Garraway and Stenholm argued that it is not necessary to achieve a spatial splitting in the interaction region if the spin states can be separated in momentum space.^{8,9} They showed that it is in principle possible to achieve this separation even for charged particles by using a small diameter of the particle beam in

the field region and a sufficiently long propagation time in an interaction free region afterwards, during which the difference in the momentum direction can lead to spatial splitting of the beam. These conditions may be fulfilled in laser-plasma experiments, where the size of the field region relates to the focus size of the laser beam, i.e., is of the order of only 10 μm (cf. inset of Fig. 7). Thus, an observation of polarized beams from laser-induced plasmas could settle the long-standing discussion whether the Stern-Gerlach effect is also measurable for charged particles.

Laser-induced generation of polarized ion beams would also be of high importance for research with particle accelerators. In this context, $^3\text{He}^{2+}$ ions have been widely discussed.¹⁰ They can serve as substitute polarized neutron beams, since in a ^3He nucleus the two protons have opposite spin directions and the spin of the nucleus is carried by the neutron. However, such beams are currently not available due to the lack of corresponding ion sources. A promising approach would be to use pre-polarized ^3He gas¹¹ as target material. In this case it is crucial that the ^3He atoms preserve their polarization during the laser-heating. This requires both electrons to be removed within picoseconds since the polarization relaxation time decreases significantly once a single electron is removed from the atom.

Polarization conservation of ^3He ions in plasmas is also crucial for the feasibility of proposals aiming at an efficiency increase of fusion reactors by using polarized fuel,¹² since this efficiency strongly depends on the cross section of the fusion reactions.^{13,14} For example, the cross sections of the dominant fusion reactions $^3\text{He}(d, p)^4\text{He}$ and $^3\text{H}(d, n)^4\text{He}$ can be increased by a factor of ~ 1.5 by the use of polarized fuel. Therefore, the energy output of fusion reactors (magnetic confinement or inertial fusion) might be increased up to one order of magnitude.

^{a)}Present address: European XFEL GmbH, WP-75, Albert-Einstein-Ring 19, 22761 Hamburg, Germany.

^{b)}Electronic mail: m.buescher@fz-juelich.de

^{c)}Present address: Leibniz-Rechenzentrum, Boltzmannstr. 1, 85748 Garching, Germany.



The present work aims at a first polarization measurement of few-MeV protons accelerated in a laser-induced plasma, which are most easily generated by using thin foil targets. A first version of the setup that was developed for such polarization studies, comprising a secondary scattering target for the laser-accelerated protons, is described in Ref. 15. For the measurements presented here an optimized, more compact version of the polarimeter was used (Sec. II). By comparing the measured differential cross section of the secondary scattering reaction with data from literature the applicability of laser-driven sources for measurements of hadronic cross sections is demonstrated. Numerical simulations with a 2D particle-in-cell (PIC) code are performed to calculate the magnetic fields and field gradients in the plasma for our target configuration in order to estimate their effect on the proton polarization (Sec. IV).

II. EXPERIMENTAL DETAILS

The measurements were carried out at the Arcturus laser laboratory at the Heinrich-Heine University Düsseldorf, where a $100 + 200$ TW Ti:Sa laser is currently in operation. Laser pulses with a typical duration of 25 fs can be produced at a rate of 10 Hz and focused on a target, where an intensity of several 10^{20} Wcm $^{-2}$ is reached. The laser was directed under an incident angle of 45° on a gold foil target of $3 \mu\text{m}$ thickness and a lateral size of a few mm. The energy that was delivered on the target amounts to ~ 1.5 J, the intensity profile at the focal point was of Gaussian shape with a width of $5 \mu\text{m}$ (FWHM).

First, the proton energy distribution was determined with the help of a permanent dipole spectrometer.¹⁶ As expected for Target Normal Sheath Acceleration (TNSA),¹⁷ an exponential fit describes the data in the region around 3 MeV, where the polarization measurements are carried out, while the maximum proton energy amounts to ~ 10 MeV. The latter value is in good agreement with experimental data found in literature, obtained at similar laser and target parameters, for example, by Zeil *et al.*¹⁸

In order to measure the polarization of the proton bunches, the spin dependence of elastic proton scattering off nuclei is employed. While the differential cross section

$d\sigma/d\Omega(\vartheta)$ describes the probability for a scattering process into a solid angle $d\Omega$ under a scattering angle ϑ , the analyzing power $A_y(\vartheta)$ is a measure for the asymmetry of the angular distribution along the azimuthal angle ϕ for a given transversal beam polarization P . Silicon is well suited as scattering target material at proton energies around 3 MeV since high precision data for both A_y and $d\sigma/d\Omega$ of the $\text{Si}(p,p')\text{Si}$ reaction are available from measurements at the Cologne tandem accelerator.¹⁹ These data are described in more detail in Refs. 20 and 21 and are sketched in Fig. 1.

A figure of merit for the statistical accuracy of a polarization measurement can be defined, that is inversely proportional to the statistical errors of beam polarization and background. For a measurement with high background this is proportional to $A_y \cdot d\sigma/d\Omega$, as described in Ref. 22. Based on this criterion Silicon is well suited to measure the polarization for protons with kinetic energies around 3 MeV at scattering angles between 40° and 50° .¹⁶

The setup for the polarization measurement is schematically depicted in Fig. 2. The symmetry axis of the setup can be inclined with respect to the production target normal by an angle Θ , that was varied in the range from 0° to 10° . At a distance of 3.5 cm behind the target foil a stack of three Radio-Chromic-Film (RCF) detectors with a hole of 3 mm in diameter at the center is placed for the monitoring of the particle rates. The small thickness of 0.1 mm of the first aperture is to minimize the amount of solid material since scattering of the protons at the edges may produce secondary particles. The Silicon scattering target with $24 \mu\text{m}$ thickness rests in a 1 cm thick target holder that serves as additional collimator. The proton beam to be analyzed has an angular divergence of $\sim 1^\circ$ and hits this target in an area of ~ 2 mm in diameter. Behind the scattering target, CR-39 detectors are placed, which cover scattering angles ϑ of up to 68° and the complete azimuthal range ϕ . These detectors are suitable for the low particle numbers per detector area A that are found at scattering angles above 40° . After every re-adjustment of the setup calibration measurements without the Silicon scattering target are carried out. The setup is modeled with the help of Geant4,²³ a Monte-Carlo software package for the simulation of the passage of particles through matter, in order to verify the alignment by a comparison of measurement and simulation.

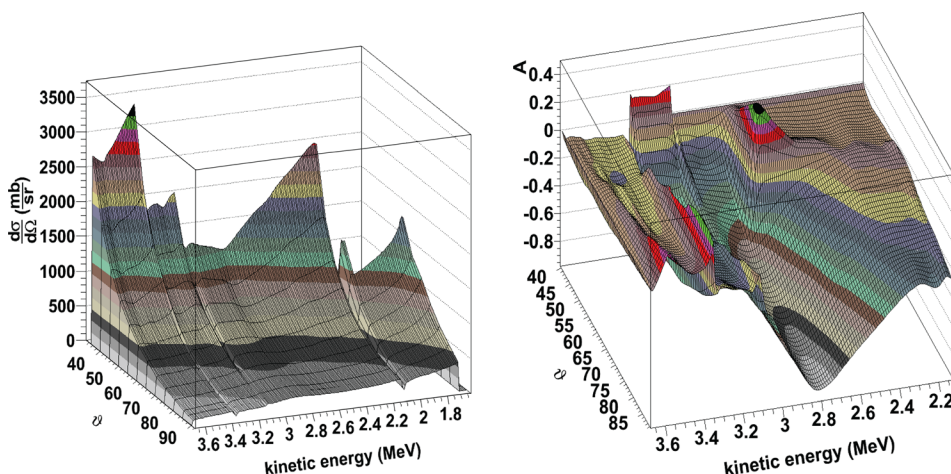


FIG. 1. Differential cross section $d\sigma/d\Omega$ (left) and analyzing power A_y (right) for the $\text{Si}(p,p')\text{Si}$ reaction in dependence of proton beam energy and scattering angle.¹⁹

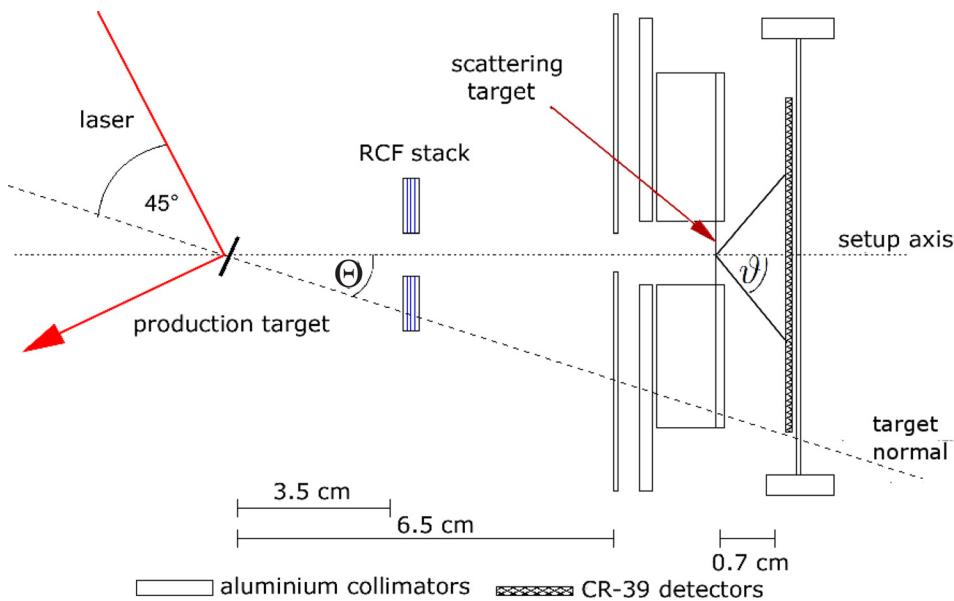


FIG. 2. Schematic view of the setup for the proton polarization measurement. For illustration purposes, the angle Θ is drawn larger than in reality.

The number of protons n_0 that impinge on the Silicon target is evaluated shot-by-shot from the dose on the calibrated RCF detectors.²⁴ Also, their energy distribution is coarsely monitored by independently evaluating the signals of the first layer dominated by 1 MeV protons, and of the second layer, whose signal corresponds to 3 MeV. Figure 3 shows microscope scans of the irradiated CR-39 detectors. Without the scattering target protons from the whole energy spectrum arrive at the detector, whereas when the scattering foil is installed those with kinetic energies below ~ 1.5 MeV are stopped in the Silicon. Within the direct beam spot the detector is overexposed and it is not possible to identify the individual tracks. However, the edge of this inner region helps to determine the position of the detector relative to the aperture.

The CR-39 detectors were etched for 24 h at 70 °C at a NaOH concentration of 7.25 mol/l. For these etching conditions, depending on the scattering angle, protons with kinetic energies of 2.6 to 3 MeV can be observed.²⁵ Combined with the exponential energy distribution at the production target this results in an energy distribution of scattered protons which can be approximated by a Gaussian shape with a mean energy of 3.2 MeV and a FWHM of 0.3 MeV. In this energy range, the number of protons arriving at the target varied between 10^6 and a few 10^8 from shot to shot.

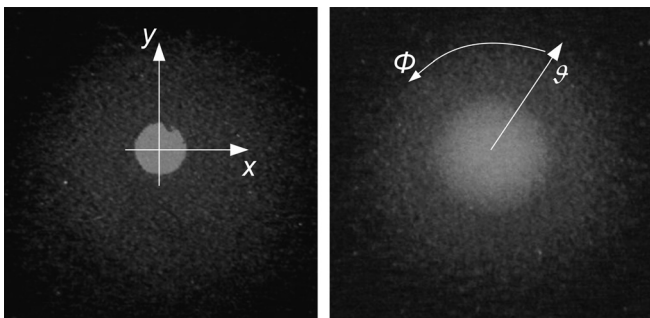


FIG. 3. Photos of two CR-39 detectors with a size of 2.54×2.54 cm without (left) and with (right) the Silicon scattering target.

For *p*-Si scattering angles $\vartheta < 37.5^\circ$ (cf. Fig. 3 for definition of coordinates and angles) multiple Coulomb scattering dominates, while at larger angles hadronic interactions become more prominent. Since the former process is an average over multiple scattering processes and thus not spin-dependent the ϕ -symmetric proton distribution below 40° is used to find the center (x_0, y_0) of each distribution. In order to minimize false asymmetries in the proton distribution along ϕ the track density n/A is evaluated for a certain choice of (x, y) . After fitting each $n/A(\phi)$ distribution by a constant function, the χ^2 of data and fit function is evaluated and the minimum χ^2 defines the true point of origin. This calibration method permits to determine the center of each distribution with an accuracy of ~ 0.02 mm.

As the next step the track density n/A is determined in dependence of the scattering angle ϑ . At scattering angles of 40° – 55° the signal on the CR-39 detectors is dominated by hadronic scattering but also contains background from impurities and scratches on the detector surface (denoted as n_{CR39}). The latter is determined and subsequently subtracted through a linear χ^2 fit of n/A in the region $\vartheta > 57.5^\circ$, where this background dominates.

After this, the areal track density is converted to the number of protons per solid angle $\Delta n/\Delta\Omega$ and the cross section is calculated according to $d\sigma/d\Omega = \Delta n/(n_0\rho_{\text{Si}}\Delta\Omega)$ using the number of incident protons n_0 from the RCF rate monitor and the areal density of the Si target ρ_{Si} . At scattering angles $\vartheta > 45^\circ$ a correction factor has to be applied, because the projection of the particle trajectories on the detector normal is already by a factor of $\sqrt{2}$ shorter, resulting in a higher minimum kinetic energy that is necessary for the proton to be detected. Figure 4 shows a comparison of $d\sigma/d\Omega$ from this work with the data from Ref. 19. Our data are an average over 10 laser shots, which corresponds to a total of $2.1 \cdot 10^9$ protons on the Silicon target. We observe a remarkable agreement between the two data sets, giving confidence both in the reliability of our data and the analysis procedures.

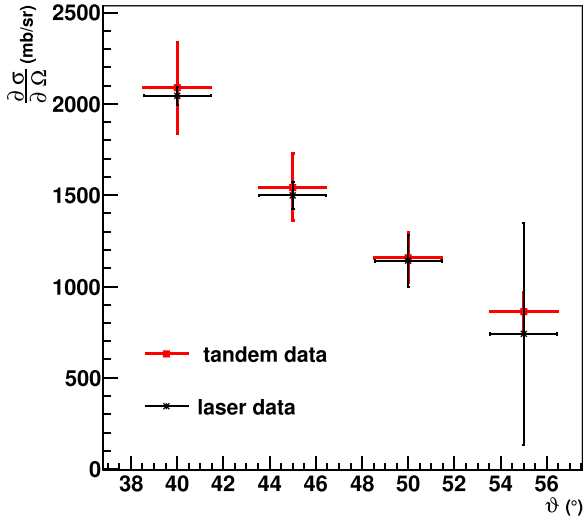


FIG. 4. Differential cross sections for the $\text{Si}(p,p')\text{Si}$ reaction at a proton energy of (3.2 ± 0.3) MeV measured at the Cologne tandem accelerator¹⁹ and from this work. The overall error of the laser data from the normalization to the RCF data amounts to 7.7% and is not included in the error bars.

III. RESULTS OF THE POLARIZATION MEASUREMENTS

For the extraction of the transversal proton polarization P the $n/A(\phi)$ distribution of the raw data (i.e., not background subtracted) is examined individually for each shot. The protons are emitted almost perpendicular to the surface of the production target with variations of few degrees. The number of protons arriving at the scattering target was between $2 \cdot 10^7$ and $3 \cdot 10^8$. In Table I we present the results for two shots (labeled #77 and #79) with their major features.

For the spin-dependent proton scattering a cosine dependence on ϕ is expected

$$N(\phi) = n_0 \rho_{\text{Si}} \Delta\Omega \left(\frac{d\sigma}{d\Omega} \right) \cdot (1 + PA_y \cos(\phi - \phi_0)) + C_{\text{CR39}}, \quad (1)$$

where $d\sigma/d\Omega$ is the unpolarized differential cross section, $A_y = -1 \dots +1$ the analyzing power, $P = -1 \dots +1$ the beam polarization, and C_{CR39} the background contribution. Since A_y varies strongly with the kinetic energy and the protons have energies in the range (3.2 ± 0.3) MeV the effective analyzing power is determined by a Monte Carlo simulation assuming $P = 1$ and by fitting the simulated data with the function given in Eq.(1).

The actual value of P is determined together with its direction, expressed by the angle ϕ_0 between the vertical

TABLE I. Summary of the two laser shots used for the polarization analysis.

	#77	#79
Proton production angle Θ	2.6°	3.8°
Number of detected protons	$2.6 \cdot 10^8$	$1.3 \cdot 10^8$
Fitted beam polarization P , ϕ_0	0.15, 217°	0.08, 80°
2 σ statistical error	0.13	0.06
Systematic uncertainty		0.08

axis and the maximum of the track density in ϕ . In order to determine P and ϕ_0 , the scanned CR-39 distributions are divided into rings of different scattering angles $\vartheta = 40^\circ - 60^\circ$ with bin widths of 5° . Each ϕ distribution is fitted by the function $n(\phi) = C_1(1 + C_2 \cos(\phi - \phi_0))$. C_1 is constrained by the differential cross section from Ref. 19 and the background n_{CR39} , while C_2 contains the known effective analyzing power A_y and the unknown degree of polarization P . For each combination of P and ϕ_0 the χ^2 between fit function and data is evaluated summarizing over all four ϑ bins. The results of the error analysis are given in Table I.

Figure 5 shows the data of shot #79 for the four different ϑ regions. In every figure the best fit of the combined data sets is shown as well as the distribution that one would expect for the same phase shift ϕ_0 and an assumed polarization of $P = 1$. The upper spectra of Fig. 5 demonstrate the importance of using ϑ regions with different signs of A_y . The distribution around 40° alone would hint at a high degree of polarization. Since the analyzing power changes its sign between 40° and 45° , in the angular region around 45° an asymmetry is then to be expected that is shifted by 180° in ϕ . The asymmetry in the $\vartheta = 45^\circ$ spectrum, however, has the same direction as at 40° . This is a strong indication that around 40° a false asymmetry is observed: according to a shot without scattering target and Geant4 simulations, a misalignment with the set-up pointing to the side of the production target can lead to asymmetric secondary scattering in the collimator to low scattering angles. This may lead to a shift of the estimated center point (x_0, y_0) and subsequently to false asymmetries at higher scattering angles. As a conservative estimate we infer a systematic error of ± 0.08 corresponding to a misalignment of 2 mm. This has to be added to the statistical errors from the χ^2 analysis. We note that the spectra for shot #77 do not exhibit the above discussed systematic asymmetry, while the individual data points show larger fluctuations leading to a higher statistical uncertainty of the fit, see Table I.

IV. COMPARISON WITH NUMERICAL SIMULATIONS

In order to estimate the magnitude of possible polarizing magnetic fields acting on the laser accelerated protons, we have carried out simulations with EPOCH,²⁶ a fully relativistic 2D PIC code. These were performed for a normally incident laser (with parameters as above) on a Au foil (thickness $2.5 \mu\text{m}$, density $6 \cdot 10^{22} \text{cm}^{-3}$, charge state 6^+) with a proton layer ($0.5 \mu\text{m}$, $2 \cdot 10^{23} \text{cm}^{-3}$). The grid size was $n_x \times n_y = 6096 \times 4048$ and the number of simulated particles $n_{\text{Au}} = 4 \cdot 10^6$, $n_p = 20 \cdot 10^6$, $n_e = 44 \cdot 10^6$, respectively.

Current PIC codes do not allow one to explicitly model the time development of the nuclear-spin degree of freedom in plasmas. Therefore, we use in the following a simplistic *ansatz* that assumes thermodynamic equilibrium. In such a scenario the efficiency of the spin-flip scenario would be governed by the Boltzmann factor

$$W(E) = \exp\left(-\frac{2\mu_p B}{k_B T}\right), \quad (2)$$

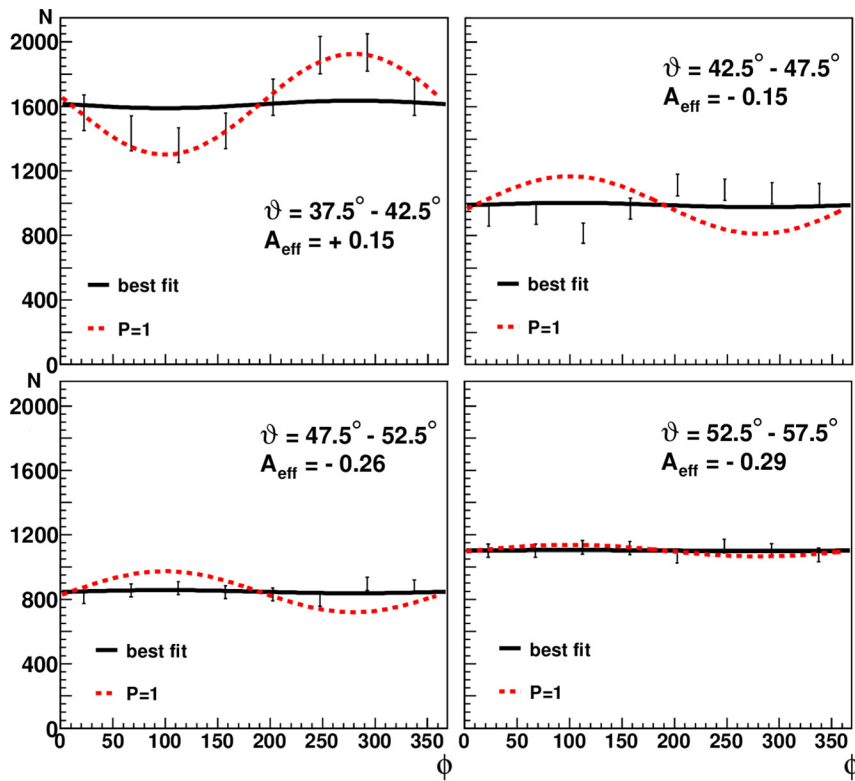


FIG. 5. Non-background subtracted data of shot #79 with the best fit for polarization P and angle ϕ_0 (black curve) and $P = 1$ (red).

where μ_p is the proton magnetic moment, and the proton temperature T is derived here from the mean kinetic energy of the protons behind the target foil. Figure 6 shows the time dependence of T as well as of the magnetic field strength B . It is seen that only at $t \sim 95$ fs do cold protons feel the influence of a strong magnetic field. This time, however, is much smaller than the typical time scale for a polarization build-up which is defined by their Larmor frequency. Thus, no significant proton polarization is to be expected since for all other times we find $2\mu_p B/k_B T \ll 1$. An efficient spin alignment would require cold targets, rapid decoupling of the accelerated protons from the heating plasma as well as large magnetic fields before the onset of heating.

As a rough estimate, a measurable spin alignment would require $2\mu_p B/k_B T \geq 1$. For room temperature ($t \leq 95$ fs in Fig. 6), $B \geq 140000$ T would be required. This field strength may be achievable in principle, however, the typical time

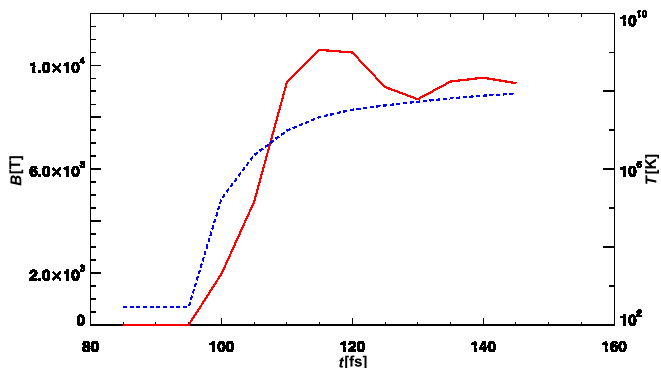


FIG. 6. Time evolution of the average proton temperature (blue dashed) and the maximum of the magnetic field strength (red solid) behind the target foil where the protons are accelerated. The laser pulse hits the foil at $t \sim 90$ fs.

that it needs to efficiently align the spins is given by the inverse of the Larmor frequency. At 140000 T it amounts to $\tau_{\text{Larmor}} = 1/(5.7 \cdot 10^{12} \text{ Hz}) \sim 170$ fs for protons, i.e., significantly longer than it takes to heat them in our case.

In order to estimate the Stern-Gerlach deflection, we then calculate the quantity

$$\alpha = \arctan \frac{\mu_p}{m_p v_x^2} \cdot \int \frac{\partial B}{\partial y} \cdot dx, \quad (3)$$

along the proton flight paths. α is an approximation for the deflection angle of a proton with magnetic moment μ_p , mass m_p , and longitudinal velocity v_x which moves through a magnetic field with gradient $\partial B/\partial y$.¹⁶ As an example Fig. 7 shows $\partial B/\partial y(x)$ at the center of the plasma where the gradients are largest. In general we find significant deflection angles only when the gradients are already sizeable at low proton velocities, i.e., at the onset of the acceleration through the electric fields. However, for all cases considered here Eq. (3) yields values of α below ~ 0.01 mrad, i.e., much smaller than the typical proton emission angles and experimental angular resolutions which both are of the order of a few degrees. Thus, no emission regions with preferred spin alignments are to be expected for the present set-up.

For both scenarios, the main argument not to expect a measurable polarization is the short time scale or the too short interaction length in which the laser-induced fields act on the particle spins. Thus, to enhance the probability of producing a polarized beam from an unpolarized target, the target size would have to be increased significantly. We therefore conclude that a target configuration with low density, like a gas jet, might be more promising than to rely on the TNSA mechanism with a foil target, although this idea

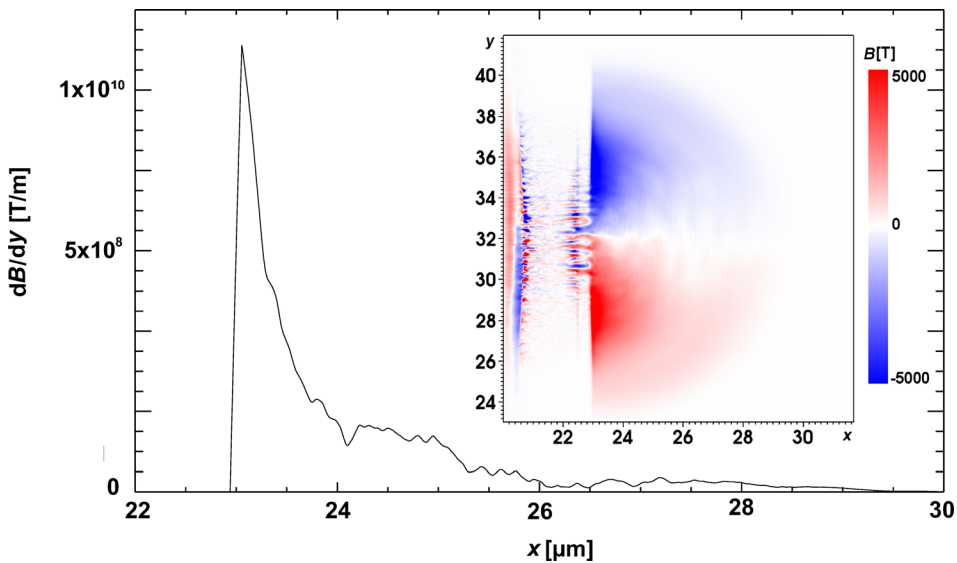


FIG. 7. Gradient of the magnetic field $\partial B/\partial y$ at $y = 32.5 \mu\text{m}$ behind the target foil (which is located at $x = 20.5 - 22.5 \mu\text{m}$ (Au) and $x = 22.5 - 23.0 \mu\text{m}$ (protons)) at $t = 120$ fs. The inset shows the underlying magnetic field distribution $B_z(x,y)$.

needs to be investigated quantitatively via appropriate simulations. In our view the most promising approach is to use pre-polarized targets, and for reasons that have been discussed in the introduction we think that ^3He gas is a good candidate.

V. CONCLUSIONS

To summarize, we have used laser-accelerated few-MeV protons to measure the scattering-angle dependence of the $\text{Si}(p,p')\text{Si}$ reaction. The result is in excellent agreement with data from literature which demonstrates the feasibility of a classical accelerator measurement with a laser-driven particle source. From the azimuthal-angle dependence of the data, the degree of polarization P of laser-accelerated protons could be determined for the first time. With the newly developed method polarizations down to $\sim 20\%$ can be detected for bunches with a sufficiently high number of produced protons ($\sim 10^8$ with energies above 2.5 MeV). As expected from computer simulations for the given target configuration, our data are consistent with an unpolarized beam $P = 0$. This finding can be interpreted such that the particle spins are not affected by the strong magnetic fields/gradients in a plasma and thus seems promising for future applications using pre-polarized targets.

ACKNOWLEDGMENTS

This work has been supported by DFG (No. GRK1203 program) as well as by Forschungszentrum Jülich (COSY-FFE). A.K. and P.Gi. acknowledge the support from the Helmholtz Alliance EMMI, as well as computing resources on grant VSR-JZAM04.

¹A. Macchi, M. Borghesi, and M. Passoni, *Rev. Mod. Phys.* **85**, 751 (2013).

²M. Borghesi, A. J. MacKinnon, A. R. Bell, R. Gaillard, and O. Willi, *Phys. Rev. Lett.* **81**, 112 (1998).

³G. Sarri, A. Macchi, C. A. Cecchetti, S. Kar, T. V. Liseykina, X. H. Yang, M. E. Dieckmann, J. Fuchs, M. Galimberti, L. A. Gizzi, R. Jung, I. Kourakis, J. Osterholz, F. Pegoraro, A. P. J. Robinson, L. Romagnani, O. Willi, and M. Borghesi, *Phys. Rev. Lett.* **109**, 205002 (2012).

⁴M. Tatarakis, I. Watts, F. N. Beg, E. L. Clark, A. E. Dangor, A. Gopal, M. G. Haines, P. A. Norreys, U. Wagner, M.-S. Wei, M. Zepf, and K. Krushelnick, *Nature* **415**, 280 (2002).

⁵A. Gopal, S. Minardi, M. Burza, G. Genoud, I. Tzianaki, A. Karmakar, P. Gibbon, M. Tatarakis, A. Persson, and C.-G. Wahlström, *Plasma Phys. Controlled Fusion* **55**, 035002 (2013).

⁶W. Gerlach and O. Stern, *Z. Phys. A: Hadrons Nucl.* **9**, 349–352 (1922).

⁷W. Pauli and S. Flügge, *Handbuch der Physik* (Springer-Verlag, 1958), Vol. 5.

⁸B. M. Garraway and S. Stenholm, *Contemp. Phys.* **43**, 147–160 (2002).

⁹B. M. Garraway and S. Stenholm, *Phys. Rev. A* **60**, 63–79 (1999).

¹⁰M. Tanaka, Y. Takahashi, T. Shimoda, M. Yosoi, K. Takahisa, and A. Plis Yu, *Rev. Sci. Instrum.* **79**, 02B308 (2008).

¹¹J. Krimmer, M. Distler, W. Heil, S. Karpuk, D. Kiselev, Z. Salhi, and E. W. Otten, *Nucl. Instrum. Methods Phys. Res. A* **611**, 18 (2009).

¹²R. M. Kulsrud, H. P. Furth, E. J. Valeo, and M. Goldhaber, *Phys. Rev. Lett.* **49**, 1248 (1982).

¹³C. Leemann, H. Buegisser, and P. Huber, *Helv. Phys. Acta* **44**, 141 (1971).

¹⁴M. Temporal, V. Brandon, B. Canaud, J. P. Didelez, R. Fedosejevs, and R. Ramis, *Nucl. Fusion* **52**, 103011 (2012).

¹⁵M. Büscher, I. Engin, P. Gibbon, A. Karmakar, A. Lehrach, T. Mennicken, N. Raab, M. Toncian, T. Toncian, and O. Willi, *J. Phys.: Conf. Ser.* **295**, 012151 (2011).

¹⁶N. Raab, “Development of a method to measure the polarization of laser-accelerated protons,” Ph.D. dissertation (Universität zu Köln, 2011), see <http://kups.ub.uni-koeln.de/4232/>.

¹⁷S. C. Wilks, A. B. Langdon, T. E. Cowan, M. Roth, M. Singh, S. Hatchett, M. H. Key, D. Pennington, A. MacKinnon, and R. A. Snavely, *Phys. Plasmas* **8**, 542 (2001).

¹⁸K. Zeil, S. D. Kraft, S. Bock, M. Bussmann, T. E. Cowan, T. Kluge, J. Metzkes, T. Richter, R. Sauerbrey, and U. Schramm, *New J. Phys.* **12**, 045015 (2010).

¹⁹B. Becker, “Data of a measurement of A_y and $d\sigma/d\Omega$ for $\text{Si}(p,p')\text{Si}$ ” (unpublished).

²⁰A. Imig, “Polarisationstransfer in der $D(d,p)^3\text{H}$ -reaktion—implikationen für astrophysik und reaktionsmechanismus,” Ph.D. dissertation (Universität zu Köln, 2005).

²¹M. Händel, “Computergestützte weiterentwicklung eines protonentransferpolarimeters für niedrige energien,” Diploma dissertation (Universität zu Köln, 1996).

²²B. Frois, J. Birchall, R. Lamontagne, R. Roy, and R. J. Slobodrian, *Nucl. Instrum. Methods* **96**, 431–436 (1971).

²³See <http://geant4.web.cern.ch> for GEANT4 Collaboration

²⁴T. Toncian, “Ultra fast laser driven micro-lens to focus and energy select MeV protons,” Ph.D. dissertation (Heinrich Heine Universität Düsseldorf, 2008).

²⁵B. Dörschel, D. Fülle, H. Hartmann, D. Hermsdorf, K. Kadnerand, and C. Radlach, *Radiat. Prot. Dosim.* **69**, 267–274 (1997).

²⁶C. S. Brady and T. D. Arber, *Plasma Phys. Controlled Fusion* **53**, 015001 (2011); see <http://ccpforge.cse.rl.ac.uk/gf/project/epoch/>.